Article

Diverging trends in large floods across Europe in a warming climate

Check for updates

Beijing Fang [1] ✉, Oldrich Rakovec [2,3], Emanuele Bevacqua [1], Rohini Kumar [2] & Jakob Zscheischler [1,4]

Large floods, which affect multiple regions simultaneously, pose substantial risks to lives and economies. In a warmer climate, increased precipitation extremes and reduced snowmelt are expected to alter flood characteristics, but how the dynamics of large floods across Europe will evolve under climate change remains unclear. By jointly assessing projected changes in the timing, spatial extent and volume of large floods in a warmer world, here we show that earlier snowmelt generally leads to earlier floods, while increasing precipitation contributions attenuate flood seasonality. Although continental-scale averages suggest limited change, they mask substantial regional heterogeneity. In western Europe, projected increases in heavy precipitation result in larger flood extents and volumes. In contrast, reduced snowmelt dominates changes in the largest floods in northern Europe, with localized shifts from snowmelt-driven to rainfall-driven floods. These regionally diverse responses of large floods to climate change should be considered in transnational flood risk management across Europe.

Flooding is one of the most destructive natural hazards, threatening lives, damaging infrastructure and disrupting communities. Widespread floods, which affect multiple basins and regions simultaneously, pose unique challenges. Their impact could exceed the sum of isolated flood events[1], particularly when they overwhelm emergency response systems, disaster relief efforts, and insurance capacities[2,3]. For instance, in July 2021, extreme rainfall caused devastating floods across multiple European countries, including Austria, Belgium, Germany, and the Netherlands, resulting in over 200 fatalities and over $54 US billion in damages[4]. This spatially compounding event overwhelmed local and regional flood management capacities and required national and cross-border coordination for both immediate response and long-term recovery. Events like this underscore the need for a targeted analysis of spatially connected flood events to improve transnational flood risk assessment and management under changing climate conditions.

The current understanding of large, spatially connected floods is still limited[5]. Most existing knowledge comes from catchment- or grid-based studies, which indicate that flood frequency, timing and magnitude in Europe have shifted in recent decades, likely in response to global warming[5–10]. Region-specific changes in flood magnitude, timing, and frequency are attributed to shifting patterns of snowmelt, rainfall, and soil moisture[7,8,10–13]. Despite this progress, the response of particularly large floods to future effects of climate change—including rising temperature, changes in precipitation variability and extremes[14], and an upward-shifting snowline—remains poorly understood, with highly varying conclusions drawn from different approaches. For instance, some studies project an overall increase for events with multi-decade return period across Europe due to intensified precipitation extremes[15]. In contrast, others project declines in similarly severe floods in northern and eastern Europe due to reduced snowmelt[16–18], as well as decreases in high flows and extreme floods in the Mediterranean region due to reduced rainfall[19,20]. These discrepancies may also be influenced by the different magnitudes of the considered floods, as floods of different rarity can be associated with different drivers and varying levels of driver extremeness[21–24]. Additionally, earlier snowmelt and shifts in flood-generating processes, such as an increase in rainstorm-induced floods, are expected to alter flood seasonality, particularly in snowmelt-dominated regions[25,26]. Overall, these studies are either constrained by uneven distributions of runoff stations or an inability to assess widespread floods across space and time, making them insufficient to gain insights about large, spatially connected floods and their underlying drivers under climate change.

An event-based approach applied to temporally and spatially consistent hydrological simulations may be able to address these limitations. In such an approach, spatio-temporally connected floods are identified through linking neighboring runoff extremes in routed runoff simulations across space and time[5,27]. Applying this approach to simulations over the historical period captured 75% of the events recorded in a flood impact

[1]Department of Compound Environmental Risks, Helmholtz Centre for Environmental Research - UFZ, Leipzig, Germany. [2]Department of Computational Hydrosystems, Helmholtz Centre for Environmental Research - UFZ, Leipzig, Germany. [3]Faculty of Environmental Sciences, Czech University of Life Sciences Prague, Prague, Czechia. [4]Department of Hydro Sciences, TUD Dresden University of Technology, Dresden, Germany. ✉e-mail: beijing.fang@ufz.de

database [HANZE,[28]]. Vice versa, about half of the 100 largest spatio-temporal floods in the model simulations, weighted by population exposure, are listed in HANZE database[5]. This shows that a spatio-temporal perspective on floods captures high-impact events.

In this study, we take an event-based approach to analyze changes in widespread European floods at 1.5 °C, 2 °C, and 3 °C of global warming relative to the preindustrial period ("Methods"). The first two warming levels were chosen to align with the Paris Agreement targets[29], while the third one is an upper bound to the projected temperature projections under current policies[30]. Using high-resolution routed runoff simulations driven by a suite of climate model simulations (Table S1), we first identify large, spatio-temporally connected flood events across Europe and then analyze

how key flood characteristics such as flood volumes and spatial extent change with warming across different regions. We further attribute projected changes in flood characteristics to shifts in the underlying flood-generating processes.

Results
Changes in frequency of large floods vary regionally

At the European scale, the average frequency of large floods—defined as events across the continent with a spatial extent above 1000 km² at any time during their lifespan ("Methods")—is projected to barely change in response to global warming (Fig. 1a). Despite negligible changes on average, uncertainties across model simulations are considerable, with some simulations
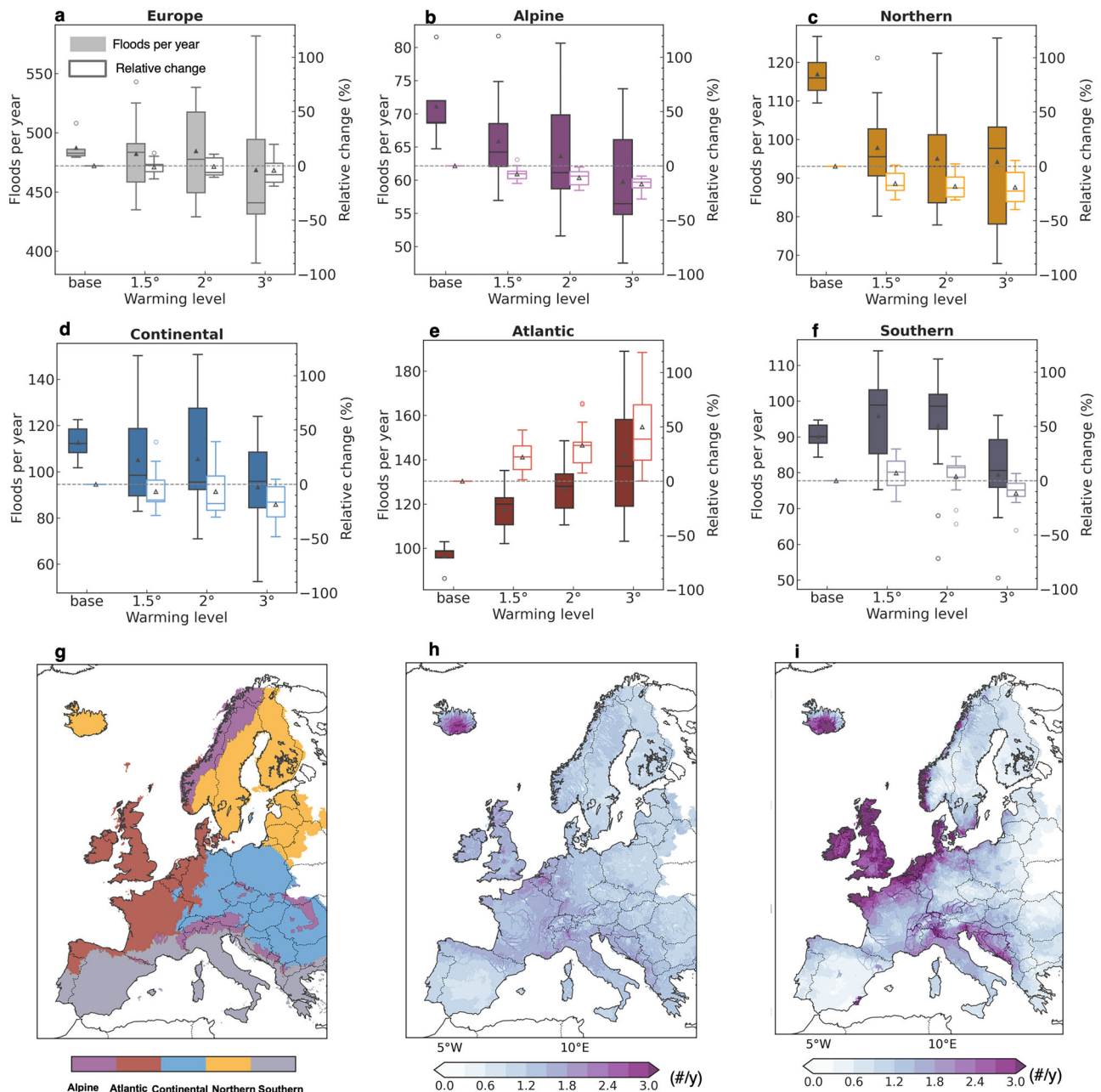

Fig. 1 | Evolution of flood frequency under different warming levels compared to the baseline period (1970–2000). a–f Filled boxes represent total number of floods per year for different regions, while hollow boxes indicate relative changes (%) compared to the baseline period. **a** Europe; **b** Alpine region; **c** Northern region; **d** Continental region; **e** Atlantic region; **f** Southern region. Boxplots display the interquartile range and whiskers show 1.5× interquartile range across model

simulations (Table S1) for different warming levels, with colors varying by region. The solid and hollow triangles represent the multi-model mean of absolute values and relative changes, respectively. Note that different ranges for the left y-axes, but the same range for the right y-axes. **g** European macro-regions used in this study. **h, i** Spatial distribution of multi-model mean flood frequency per year during the baseline period and under 3 °C warming, respectively.
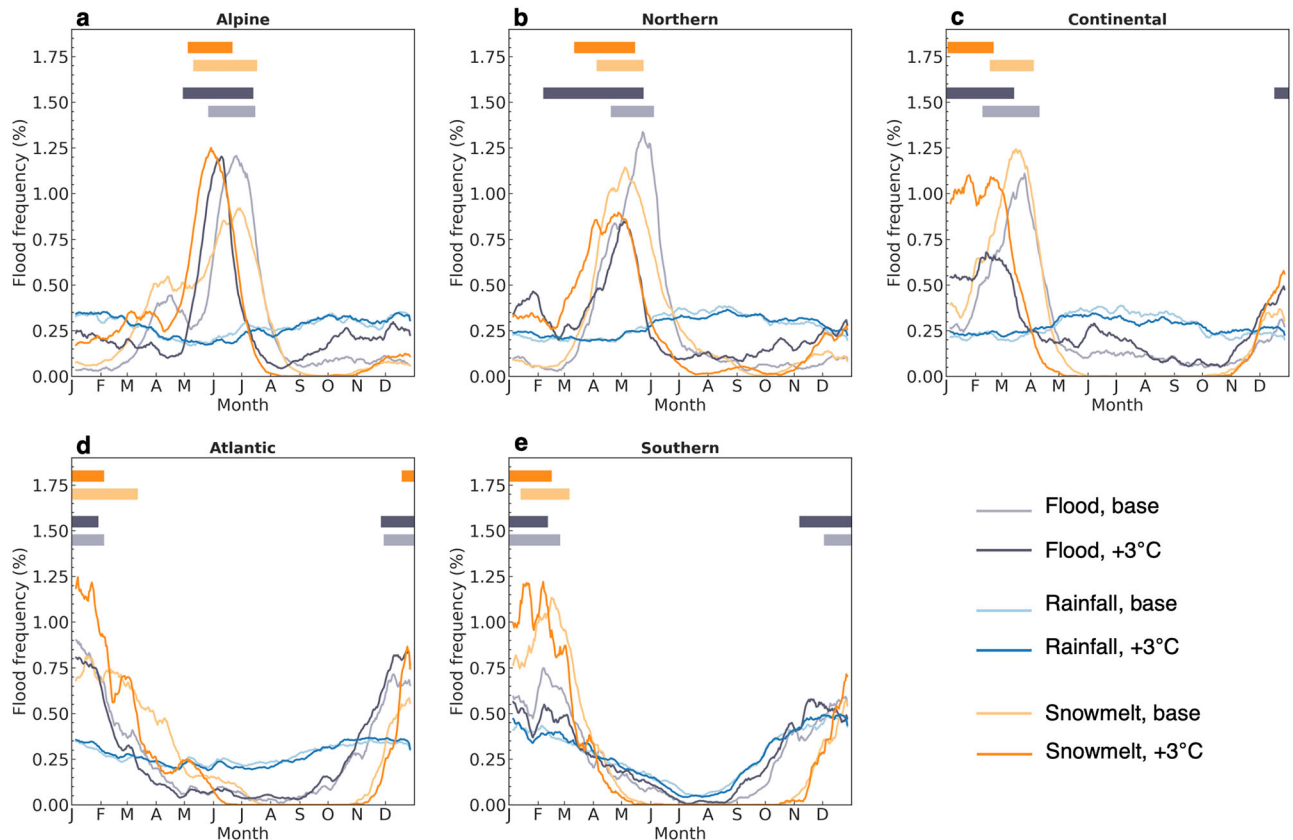
Fig. 2 | Seasonality of flood, snowmelt, and rainfall events during the baseline period (1971–2000) and under the 3 °C warming level. a–e The results are based on multi-model mean estimates for different regions. Snowmelt and rainfall events are defined, similarly to floods, as spatio-temporally connected grid cells where snowmelt or rainfall exceeds the 80th percentile of wet days (snowmelt/rainfall > 1 mm, see "Methods"). The curves denote the average percentage of detected events occurring on each day of the year, smoothed using a 10-day moving window for visual clarity. Bars indicate the main flood and snowmelt seasons, defined as the shortest continuous period capturing at least 50% of all events, for the 3 °C warming level (darker colors) and baseline period (lighter colors).

indicating a strong increase and others suggesting a strong decrease in flood frequency with future warming. When taking a regional scale perspective, distinct patterns emerge (Fig. 1b–g), with changes generally becoming more pronounced under 3 °C warming compared to 1.5 °C.

The changes in the frequency of large floods at the regional scale typically follow expected changes in the dominating flood-generating processes[5]. In snow-dependent regions, the frequency of large floods tends to decline under global warming (Fig. 1b–d), primarily due to reduced snowpack, a shorter snow season and less snowfall, despite overall increasing precipitation[31,32]. For instance, in the Alpine region, the multi-model mean flood occurrence is expected to decrease by 17% under the 3 °C warming level compared to 1971–2000. Similarly strong reductions in flood frequency of 19% are projected for Northern and Continental Europe, albeit with greater uncertainty. In contrast, flood frequencies in the Atlantic region (Fig. 1e), which is dominated by rainfall-driven floods, are projected to strongly increase by 50%, mainly driven by increasing precipitation extremes[20]. The reported changes generally intensify with increasing global warming. For instance, flood frequencies in the Atlantic regions increase by 22% in a 1.5 °C warmer world to 33% in a 2 °C warmer world, ultimately reaching the above-mentioned 50% increase in a 3 °C warmer world. Uncertainties in flood frequency projections also increase with warming. In Southern Europe, changes in flood occurrence are generally less pronounced (Fig. 1f), with a slight decrease of 12% under 3 °C warming, likely due to an overall reduction in precipitation[33,34]. Nonetheless, also in this region, the variability across model simulations is large.

A spatially explicit analysis of which areas are exposed to frequent large floods provides a more detailed picture of expected future flood patterns. Here, a higher flood frequency in a given location means a greater likelihood that the location will be part of a widespread flood (Fig. 1h, i). Under the 3 °C warming level, the most pronounced frequency increases of large floods are projected along the Atlantic region, including England, Ireland, and the western parts of France and Germany. Similar patterns but with a smaller magnitude are also identified under the 1.5 and 2 °C warming levels (Fig. S1). In contrast, decreases are expected in snowmelt-dependent regions, such as northern and eastern Europe. Interestingly, despite an overall decline in snowmelt across Europe, at the local scale, increases in flood occurrence are projected along the Scandinavian Mountains, southern Sweden, and coastal areas of the Continental area (Fig. S1a). These increases suggest that increasing precipitation extremes are likely to outweigh the reduction in snowmelt in the future, potentially shifting flood regimes from snowmelt-driven to rainfall-driven in these regions. This is consistent with detected changes in flood drivers in observed runoff data over the historical period[9].

Earlier snowmelt leads to earlier large floods

Rising temperatures lead to earlier and reduced snowmelt[25,35], which alters the timing of floods, particularly in snowmelt-dependent areas such as the Alpine, Northern, and Continental regions[5]. This occurs because in these regions flood seasonality typically mirrors the seasonality of snowmelt, with distinct periods of high and low flood occurrence (Fig. 2a–c). In contrast, the seasonality of heavy rainfall is much weaker and shows little change with warming compared to the projected changes in snowmelt seasonality. Nevertheless, changes in the relative contribution of rainfall to floods may still modulate flood seasonality in some regions, as discussed below.

To quantify changes in flood seasonality and its contributing factors, we define the main flood season as the shortest period accounting for at least

50% of all floods ("Methods"). In the Alpine region, the flood seasonality exhibits a bimodal pattern over the baseline period (Fig. 2a), reflecting the very diverse topography and large spatial coverage of the region (Fig. 1g). In line with the importance of snowmelt for flood occurrences[25], the bimodal pattern is also visible in the snowmelt seasonality. In the Carpathians and Dinaric Alps, the first flood peak in early spring is primarily driven by snowmelt in the baseline period (Fig. 3a). Under 3 °C warming, the spring flood peak weakens, as the rising snowline reduces spring snowmelt (Figs. 3b, c and 2a). In the Scandinavian part of the Alpine region, where summer floods (June to mid-July) have historically been dominant, earlier snowmelt under warming shifts the flood onset to May, while the end of the flood season remains unchanged.

In the Northern region, the flood seasonality is projected to strongly attenuate under 3 °C warming due to reduced snowmelt seasonality and increased rainfall contributions (Fig. 3g–i and S2b). In the reference period, the primary flood season spans late April to May (Fig. 2b). Under 3 °C warming, this season expands, by starting two months earlier and ending only slightly sooner, resulting in a much longer overall flood season. This indicates that the advancement of flood timing observed historically in this region[7,36] is projected to continue in the future. Additionally, a secondary peak emerges in January and February, which is driven by an increased proportion of winter snowmelt and enhanced winter rainfall-induced floods in areas such as southern Sweden, Lithuania, Latvia, and Estonia (Fig. 3g–i and S2b).

A similar weakening of flood seasonality and earlier flood timing is projected for the Continental region, where the primary flood season shifts from early spring to late winter (Fig. 2c). This shift is also driven by strongly decreased snowmelt-induced spring runoff and increased rainfall contributions (Fig. 3g–i and S2c). In contrast, only small changes in flood seasonality are expected in the Atlantic region and Southern Europe, where flood generation is dominated by winter precipitation, resulting in low sensitivity to changes in snowmelt seasonality (Fig. 2d, e). However, with the substantial increase in flood frequency in the Atlantic region (Fig. 1e), a corresponding rise in winter floods is expected in the future (Fig. S2d).

Changes in the timing of large floods generally align with changes in snowmelt timing across space for many regions (Fig. 3c, f). In the Alpine region, 56% of the area is expected to experience mean snowmelt timing 15–30 days earlier under 3 °C warming, resulting in a similar shift in flood timing across 28% of the area. In parts of the southern Scandinavian Mountains (Fig. 3a, b), flood timing is expected to shift from summer to winter, in line with a transition from snowmelt- to rainfall-driven flooding regimes (Fig. 3g, h). In the Northern region, the shifts are even more pronounced. About 81% of the area is expected to experience snowmelt 30–45 days earlier, with 53% of the area experiencing an associated shift towards earlier floods by 30–60 days. On average, flood timing across this region is expected to advance by 38 days (Fig. S3b). The most substantial changes are expected around the Baltic Sea (Fig. 3c), particularly in southern Sweden and southern Finland. Parts of the Baltic coastline and Iceland are projected to shift towards a winter rainfall-driven flooding regime (Fig. 3h, i). In the Continental region, flood and snowmelt timing shifts are largely consistent (Fig. S3c), but more dispersed compared to the Alpine and Northern regions. Here, 88% of the area is projected to experience earlier snowmelt timing, with 55% showing earlier flood timing by 10–40 days. In contrast, 22% of the region is expected to exhibit later flood timing (Fig. 3c). The diversity in flood timing changes in the Continental region arises from its mixed flood-generating processes, with large areas experiencing the dominant regime shifting from snowmelt-driven to rainfall-driven flooding (Fig. 3g–i). Generally, no strong shift in mean flood timing is observed in the Atlantic and Southern regions. Overall, the changes are similar but of smaller magnitude under the 1.5 °C and 2 °C warming levels (Figs. S3d–i and S4).

Differences in changes of flood extents across magnitudes
The spatial extent of widespread large floods is critical for impacts, for instance, to the population and financial assets. Similar to changes in the frequency of large floods, the spatial extent shows little change at the European scale (Fig. 4a). However, flood responses vary across magnitudes.

Specifically, moderately large floods (0th–50th percentile of all detected floods) exhibit minimal changes, while severe floods (50th–95th percentile) expand by up to 10% under 3 °C warming. In contrast, the most extreme floods (above the 95th percentile) do not change much with warming. This nonlinear response across flood magnitudes emerges from strongly pronounced patterns at the regional scale, except in the Atlantic region. For instance, in the Alpine region (Fig. 4b), severe floods are projected to grow more (15–40%) than the most extreme floods (around 10%), despite a general expansion across nearly all percentiles. Along with a decline in frequency (Fig. 1), this suggests fewer but more widespread floods in the future. A similar pattern is observed in the Continental region, where moderately large and extreme floods show negligible changes, while severe floods expand by up to 20%.

In the Northern region, the most extreme floods exhibit opposite responses compared to severe floods (Fig. 4c). While severe floods are projected to expand up to 20% under the 3 °C warming level, the most extreme floods are expected to substantially decrease in extent (Fig. 4f). In particular, the median size of top 100 floods (around 97th percentile; Table S2) by extent is projected to significantly shrink by 33% ($p < 0.05$, Fig. S5c). In contrast, in the Atlantic region, there are barely any changes projected in flood extent across all magnitudes, with only a slight expansion for very extreme floods. However, the top 100 floods show a significant 21% increase under the 3 °C warming level compared to the baseline period ($p < 0.05$, Fig. S5e), indicating that the most extreme floods in the Atlantic region will become both more frequent and more extensive. In the Southern region, flood extents are projected to decrease by over 20% for most flood magnitudes, but the extent of extremely large floods remains nearly unchanged relative to the baseline period, warranting continued attention. These highly variable responses of flood extent across flood magnitudes and regions highlight the need for targeted flood adaptation strategies, particularly for the severe floods which are expected to change the most. Lower warming levels are generally associated with smaller changes. For instance, limiting warming to 1.5 °C would nearly halve the expansion of severe floods in the Alpine region compared to the 3 °C warming level (Fig. 4b), highlighting the benefits of stringent climate mitigation efforts.

Larger flood volumes driven by increased precipitation
Flood volume, which integrates flood extent, duration, and intensity, provides a comprehensive perspective on flood risk. To understand the drivers of changes in flood volume, we further analyzed variations in rainfall and snowmelt contributions under different warming levels ("Methods", Fig. 5). Note that, on average in our simulations, approximately half of the precipitation and snowmelt turns into runoff, with the remainder lost to evapotranspiration or stored within soil or groundwater systems. Across flood magnitudes, combined rainfall and snowmelt volumes explain more than 80% of the flood volume in all regions and warming levels, suggesting that flood volume changes can be investigated by analyzing changes in flood drivers.

At the continental scale, flood volume remains stable across warming levels due to compensating effects of increased precipitation and reduced snowmelt (Fig. 5a). However, regional patterns reveal notable differences. In snow-dependent regions, such as the Alpine and Continental regions, despite the decrease in flood occurrence, the decline in snowmelt contributions is largely offset by a substantial increase in precipitation contributions at the event scale, leading to an overall rise in flood volume across magnitudes (Fig. 5e, j), particularly for severe floods (50th–95th percentile). Specifically, median flood volume increases slightly by 15% in the Alpine region ($p < 0.05$, Fig. 5b) and 11% in the Continental region ($p > 0.05$, Fig. 5g), driven by a strong rise in rainfall contributions (58% and 68%, respectively), which compensates for the sharp decline in snowmelt contributions (21% and 30%, respectively). Severe floods show even greater increases, reaching up to 30% in both regions. In contrast, the changes in extreme floods in the Northern region are dominated by a strong decline in snowmelt. Focusing on the top 100 events by volume (Fig. S6), the mean (median) flood volume decreases significantly by 35% (39%) due to sharp reductions in snowmelt contributions (54% in mean, 65% in median).

Notably, under the 3 °C warming level, rainfall contributions are projected to surpass snowmelt contributions, highlighting a shift in the flood generation regime in this region.

Rainfall-dominated regions exhibit varied responses due to differences in projected changes in precipitation, with the Atlantic region warranting special attention. While the median flood volume remains largely
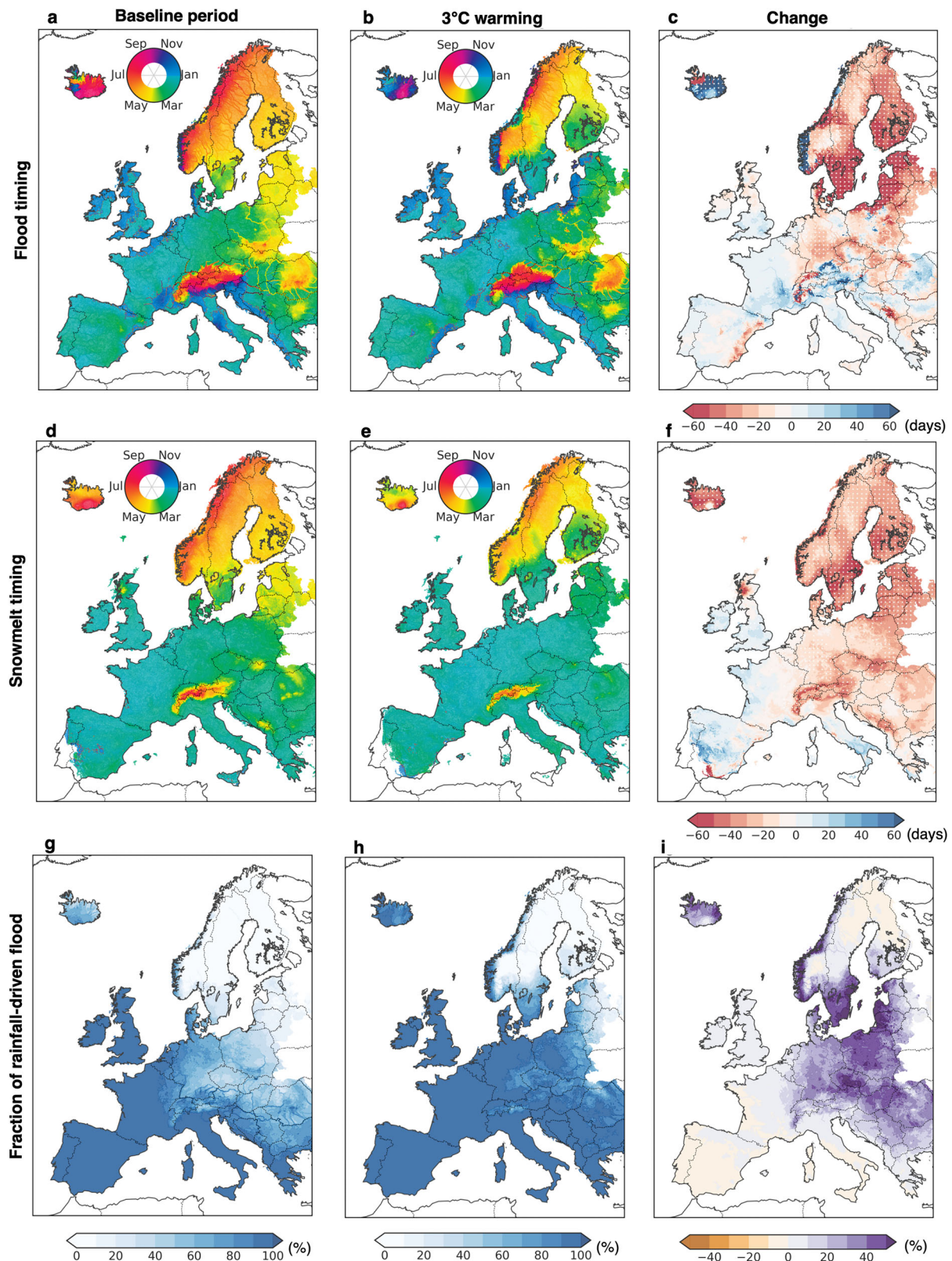

Fig. 3 | Spatial distribution of flood and snowmelt timing and the fraction of rainfall-driven events. a–c Spatial distribution of the average timing of flood events for each grid cell during the baseline period (1971–2000 (**a**)) and under the 3 °C warming level (**b**), along with the changes between these periods (**c**). **d–f** the same with (**a–c**), but for snowmelt event timing. White dots in **c**, **f** indicate significant changes in mean timing (Watson–Williams Test, two-sided, $p < 0.05$) with over 50% model agreement. Spatial distribution of the fraction of rainfall-driven floods during the baseline period (**g**), under the 3 °C warming level (**h**), and the relative changes between these periods (**i**).
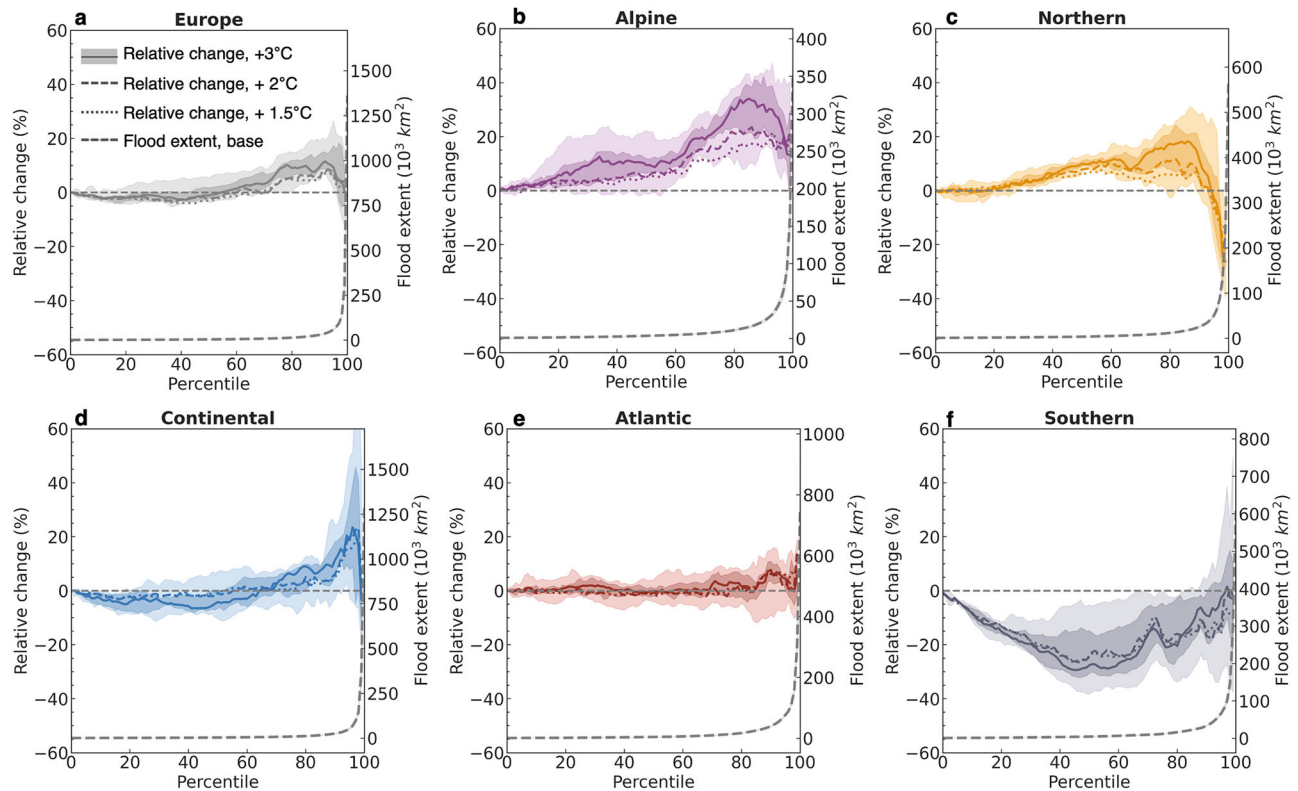
Fig. 4 | Evolution in flood spatial extent across different magnitudes under different warming levels. a–f Relative changes (%) of flood extent under 1.5 °C, 2 °C, and 3 °C warming compared to the baseline period across different quantile levels. Lines represent the median values across model simulations. Solid/dashed/dotted lines denote 3 °C/2 °C/1.5 °C warming, respectively. The darker shading indicating the 25th–75th percentile range and lighter shading showing the minimum-maximum range for the 3 °C warming. Dashed gray lines depict the historical distribution of flood extents (unit: 1000 km²). The legend in **a** is common to all panels (**a–f**), with colors varying by region.

unchanged in this region, the mean (median) volume of the top 100 largest events increases significantly by 34% (37%), driven by a substantial rise in rainfall contributions (+39% in mean, +35% in median), associated with intensified extreme rainfall[37] (Fig. S6). In the Southern region, flood volume changes generally align with flood extent patterns, showing strong decreases for moderately large floods but little change for severe and extreme floods.

Changes in the combined rainfall and snowmelt contributions across percentiles align well with changes in flood volume, suggesting that runoff efficiency remains relatively consistent across flood severity (Fig. 5d–f, j–l). An exception occurs in the Atlantic region (Fig. 5k), where flood volume increases slightly more than the combined rainfall and snowmelt volumes, implying enhanced runoff efficiency under 3 °C warming level compared to the baseline period.

Discussion

This study systematically examines the future evolution of large European floods from an event-based perspective by considering spatiotemporally connected runoff extremes. The approach allows us to integrate flood extent, total volume and seasonality alongside frequency. Understanding changes in the characteristics of widespread floods is important to improve water resource and flood risk management, as most societal impacts are caused by spatially extensive floods (Fig. 6 and S7–8 for 1.5 °C and 2 °C warming levels).

Limited changes in large flood occurrence or magnitude are projected on average at the European scale, as continental averages mask substantial regional heterogeneity. For instance, in the Atlantic region, floods are projected to become more frequent, extensive and intense. In particular, the top 100 flood events by volume in this region are expected to increase by 34% in volume and 33% in spatial extent, driven by a 39% increase in contributing precipitation. Such a growing threat from the most extreme

floods, which likely exceed basin-scale flood management and even national planning capacities, underscores the need for regional and continental cooperation in flood risk management.

In snow-dependent regions such as the Alpine, Northern, and Continental regions, flood occurrence is expected to decline due to a substantial reduction in snowmelt. However, reduced frequency does not eliminate flood risks. The Alpine region, for instance, is projected to experience fewer but more widespread floods. In contrast, the Northern region exhibits a more complex pattern: severe floods are projected to become more extensive, while extreme floods are expected to decrease significantly in both extent and intensity. Such nonlinear and even opposing changes in severe and extreme floods in the Northern region may be linked to similar patterns in snowmelt behavior. In this region, moderate snowmelt events tend to expand, while the most extensive events shrink due to declining snowpack, contributing to a reduction in the most extreme floods in this snowmelt-dependent region. Overall, this varied response across flood magnitudes, along with the overall spatial heterogeneity of changes, aligns with previous studies[16,19,20,38,39], while offering a more nuanced and comprehensive understanding of the evolution of particularly large floods.

Our results on changes in flood timing confirm that earlier snowmelt advances flood timing, consistent with previous studies[25]. Additionally, we identify a shift in the flood-generating regime from spring snowmelt-driven to winter rainfall-driven in parts of the Alpine (e.g., southern Scandinavian Mountains), Northern (e.g., southern Sweden), and Continental regions. This transition is mainly driven by reduced snowmelt, an upward-shifting snowline, and increased precipitation[40,41].

We also acknowledge that non-climatic factors, particularly urbanization and deforestation, can substantially influence flood risks beyond the physical drivers analyzed. Urban expansion can intensify flooding[42] and reduce flood response times[43] by expanding impervious surfaces[44] and
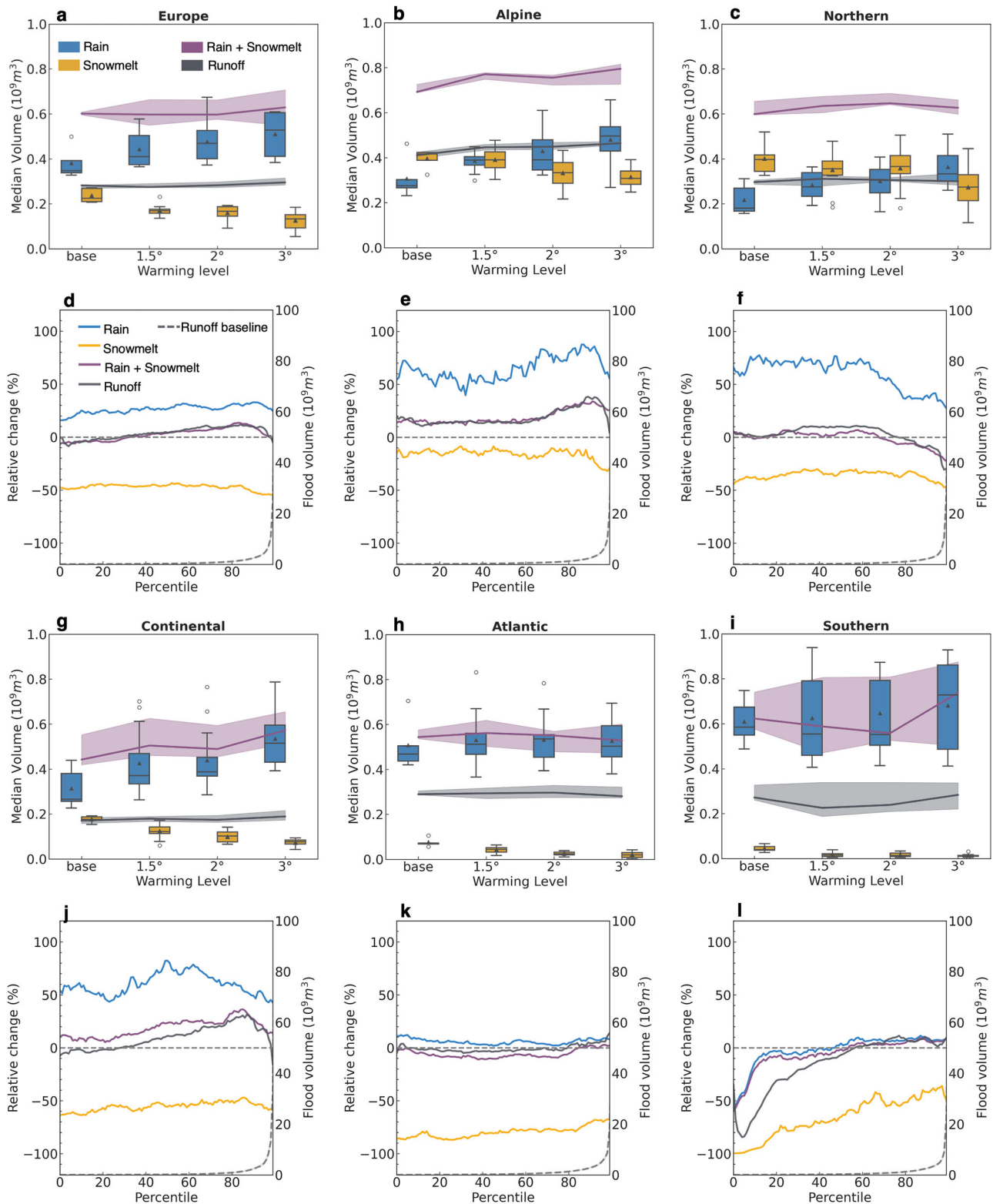
Fig. 5 | Evolution of flood volume under different warming levels and their contributing factors. a–c, g–i Median flood volumes and their contributions from rainfall (blue box) and snowmelt (yellow box) under varying warming levels for Europe and all subregions. Purple lines represent the combined volume of rainfall and snowmelt contributing to median floods, while gray lines indicate the total generated runoff volume, considered as flood volume. Lines show the median values among model simulations, with shading indicating the interquartile range. Blue and yellow boxes represent the absolute volumes of contributing rainfall and snowmelt. Boxplots indicate the interquartile range, with whiskers extending to 1.5× the interquartile range across model simulations. **d–f, j–l** Relative changes of flood volume (gray lines), rainfall contribution (blue lines), snowmelt contribution (yellow lines) and the combined volume of rainfall and snowmelt (purple lines) under the 3 °C warming level compared to the baseline period, for different percentiles (Methods). Lines represent the median values across model simulations. Dashed gray lines denote the historical distribution of flood volumes over the baseline period.

		Frequency	Extent	Volume	Rain_Vol	Snow_Vol	Mean Timing
Alpine	**All**	-17%	+ 10% (+21%*)	+15%* (+23%*)	+70%*(+59%*)	-40%*(-25%*)	- 15~30 days (28% cells)
	Top 100		+8% (+2%)	+12% (+8%)	+49%*(+35%*)	-81%*(-37%*)	
	Flood risks	Less frequent, but more widespread and larger floods.					
Northern	**All**	-19%	+10% (-4%)	+8%* (-13%)	+86%*(+32%*)	-46%*(-44%*)	- 30~60 days (53% cells)
	Top 100		-34%* (-32%*)	-39%*(-35*%)	2%(-7%)	-65%*(-54%*)	
	Flood risks	Fewer floods, with severe floods intensifying but extreme floods weakening.					
Continental	**All**	-19%	-3% (+8%)	+11% (+9%)	+76%*(+41%*)	-81%*(-59%*)	-10~40 days (55% cells)
	Top 100		53% (-7%)	-3% (-14%)	+12%(+11%)	-63%*(-69%*)	
	Flood risks	Fewer floods, with severe floods becoming slightly more intense.					
Atlantic	**All**	+50%	-1% (+3%)	-2% (+6%)	+4%(+8%)	-99%*(-73%*)	Insig.
	Top 100		+36%*(+33%)	+37%*(+34%*)	+35%* (+39%*)	-65%* (-60%*)	
	Flood risks	Much more frequent floods, and extreme floods become more extreme.					
Southern	**All**	-12%	-24%* (-8%)	-9% (+7%)	0%(+10%)	-99%*(-51%*)	Insig.
	Top 100		-4%(-8%)	-2%(+5%)	+5%(+7%)	-55%*(-40%*)	
	Flood risks	Fewer floods, with severe floods weakening while extreme floods remain stable.					

Fig. 6 | Summary of changes in future flood risks under the 3 °C warming level compared to the baseline period (1971–2000) for different European macroregions. Rain_Vol and Snow_Vol denotes the contributions from rainfall and snowmelt to floods, respectively. In the Extent, Volume, Rain_Vol, and Snow_Vol columns, values outside parentheses indicate relative changes in median statistics, while values inside parentheses represent mean statistics. Asterisks (*) denote statistically significant changes based on a median test (for medians, two-sided) or Student's t-test (for means, two-sided) at the 0.05 significance level, with over 50% model agreement. Entries with either a significant median or mean change with a consistent sign are highlighted in color. To ensure consistency within the table, the top 100 flood events are all ranked by flood volume. Additionally, the relative change in median Rain_Vol and Snow_Vol for all/top 100 events is calculated by pooling the corresponding data samples, rather than using values from the median flood alone (as shown in Fig. 5a–c, g–i).

altering surface roughness[45]. Deforestation can also alter both rainfall patterns and infiltration capacity, creating shifts in runoff generation that vary across spatial and temporal scales[46].

The robustness of our findings largely depends on the climate models used, the performance of the hydrological simulations, and the flood detection method. We employed five climate models from the Coupled model Intercomparison Project Phase 5 (CMIP5[47]), which are also used in the impact model simulations of the Inter-Sectoral Impact Model Intercomparison Project (ISIMIP[48]) to cover a broad range of temperature and precipitation projections[49]. These datasets were bias-corrected and further downscaled to a 5 km resolution across Europe using a trend-preserving external drift kriging method[50]. This approach enables high-resolution hydrological modeling, which is critical for the event-based flood detection methodology employed in this study. While the more recent generation of climate models (CMIP6) offers finer resolution and improved physics, spatial patterns of flood changes and associated risks have been shown to remain largely similar to CMIP5[20,51,52]. Nonetheless, some CMIP6 models show improvements in the representation of extreme precipitation[53,54]. Therefore, while the spatial trends may be similar, differences in the magnitude of projected flood changes may still arise. In addition, notable model uncertainty is evident in projected flood occurrence and other characteristics, as reflected in the wide spread of model results, especially under the 3 °C warming scenario. Although significance testing and model agreement are explicitly shown, the ensemble spread highlights the importance of interpreting these results with caution.

With regard to hydrological modeling, although mHM runoff simulations effectively reproduce observed indicators, uncertainties remain, particularly in semi-arid regions and lake-dominated areas such as Southern Finland[5,19]. Moreover, although the flood detection parameters have only a minimal influence on the identified flood database[5], some attribution-related limitations persist. By restricting contributing runoff, rainfall, and snowmelt to the seven days preceding and during floods, potential prior contributions from earlier events or changes in soil moisture might be excluded. Contributions from groundwater and boundary effects could also marginally influence results. Additionally, this study mainly focuses on widespread fluvial floods with potential spatially compounding impacts, while flash floods, pluvial events, and coastal compound floods are not considered.

The findings of our study have important implications for European-level policy frameworks, particularly the EU Floods Directive[55] and transboundary flood management strategies. The pronounced regional heterogeneity in projected large flood responses highlights the need to move beyond traditional catchment-scale approaches toward coordinated flood risk management at regional and transnational levels. This should be supported by cross-border collaboration in infrastructure planning, early warning systems, and emergency preparedness[3,8,56,57]. In regions where flood magnitudes and frequencies are projected to increase substantially—such as the Atlantic region-adaptive infrastructure planning and revised flood zoning regulations will be essential[58]. Meanwhile, regions facing shifts in flood timing or reduced snowmelt-driven floods, such as the Alpine and Northern European regions, will require updated reservoir operation guidelines, water resource management strategies, and agricultural planning to accommodate changing hydrological conditions[31,35]. Integrating these region-specific insights into the implementation and revision processes of the EU Floods Directive can strongly enhance Europe's collective resilience to future flooding under climate change. Furthermore, our findings also confirm that restricting warming to 2 °C could substantially mitigate flood risks in the densely populated regions of Europe, such as the Atlantic region, reducing the projected flood occurrence increase from 50 to 33% and leading to decreases in flood extent and volume. Our results highlight the importance of climate mitigation and adaptation efforts to minimize future impacts of very large floods.

Methods

Data

Daily routed runoff simulations over Europe were derived from the mesoscale Hydrologic Model (mHM)[59,60], forced by five CMIP5 general circulation models (GCMs: HadGEM2-ES, IPSL-CM5A-LR, MIROC-ESM-CHEM, GFDL-ESM2M, and NorESM1-M) from Inter-Sectoral Impact Model Intercomparison Project (ISIMIP) under three Representative Concentration Pathways (RCPs 2.6, 6.0, and 8.5) from 1950 to 2099. The mHM model has been proven to effectively reproduce observed indicators and capture widespread floods[5,19], despite some limitations in semi-arid regions and lake-dominated areas. Precipitation and temperature data from the models were downscaled and bias-corrected to a spatial resolution of 0.5° using a trend-preserving approach[61], then further interpolated to 5 km for Europe within the EDgE project (ref. 50; http://edge.climate.copernicus.eu/) using external drift kriging. These high-resolution climate data were finally fed into the mHM model for flood detection[62,63]. Note that the snowmelt data derived from mHM were used for flood classification and change attribution. Additionally, the subdivision of five European macro-regions (i.e., Alpine region, Northern region, Continental region, Atlantic region and Southern region) following refs. 64–66 was used for regional analysis.

Identification and characterization of flood events

We use the peak-over-threshold method to identify the large spatio-temporally connected flood events. Specifically, floods at the grid cell level are defined as days in which daily runoff exceeds the local 99th percentile, referenced to the 1971–2000 period. Flood patches for each day are identified by grouping spatially connected flood grid cells that share an edge or vertex. We then calculate the overlap ratio between flood patches across two consecutive time steps. If the ratio of the overlapping area to both of the previous and current patches exceeds 0.4, the time steps are merged into a single event (for more details, see ref. 5). Note that, to focus on widespread floods and exclude non-riverine floods, we consider only flood events that include at least one grid cell of a main stream (i.e., a river with a catchment area larger than 1000 km^2). Additionally, for each time step, the spatial extent of flood patches must exceed 1000 km^2. Based on the identified spatio-temporal flood events, key characteristics-including timing, extent, and volume-were quantified. Timing is defined as the onset date of the flood event, extent refers to the total affected area. Flood volume is defined as the total runoff generated within the hydrological catchment during the seven days preceding flood onset until the event's end date. The seven-day window was chosen as it is considered sufficient for response times in large catchments[67] and is widely used in flood attribution analyses[7]. Sensitivity analyses using five-day and ten-day windows yielded consistent results (Figs. S9–12), confirming the robustness of the main findings. The hydrological catchment for each flood event is defined as the combined upstream catchments of all grid cells included in the event. The main results of this study remain robust against slightly different choices of the flood detection parameters.

To examine changes in flood characteristics under climate change, we use 1971–2000 as the baseline period representing the recent climate. Future conditions were represented by 30-year periods corresponding to 1.5 °C, 2 °C, and 3 °C global warming levels relative to the preindustrial period. Detailed information on the selection of these 30-year periods and their specific values for each model and scenario can be found in Marx et al.[65]. Specifically, combining different GCMs and Representative Concentration Pathways (RCPs), there are 5 model simulations for the baseline period, 14 simulations for the 1.5 °C warming level, 13 simulations for the 2 °C warming level, and 8 for the 3 °C warming level (Table S1).

Attribution of shift in flood timing

To explore the drivers of the changes in flood timing, we compared flood timing with the timing of heavy rainfall and snowmelt events. Rainfall and snowmelt events were identified similarly to flood events but using the 80th percentile of wet days (rainfall/snowmelt > 1 mm) as the exceedance threshold. This includes heavy, though not only extreme, rainfall and snowmelt events.

The timing of these events was analyzed from both an event-based and a grid-based perspective. On an event basis, as described above, the onset date was used as the event's timing. For each sub-region in Europe under a given warming level, event onsets were summarized as the mean occurrence probability for each day of the year across different model simulations. On a grid basis, we assigned each grid cell within an event with its earliest start date. These start dates were then averaged over all events in each grid cell using circular statistics[68]. Finally, we compared flood timing with rainfall and snowmelt timing under different warming levels. The significance of the changes in mean flood/snowmelt timing under different warming levels were assessed using Watson–Williams test.

Attribution of changes in flood magnitude

To provide a more complete picture of how flood event spatial extent and volume may change in the future, and to assess whether these changes are consistent across different magnitudes, we examine changes in flood extent and volume for different percentile levels. Specifically, for each warming level 1.5 °C, 2 °C, and 3 °C, we calculate the relative change of flood extent relative to the baseline period across different percentile levels.

To identify the drivers of flood volume changes under climate change, we quantify the contributions of precipitation and snowmelt to flood events and compare them with total flood volume. Specifically, rainfall and snowmelt contributions are calculated as the respective volumes generated within the hydrological catchment during the seven days preceding the flood onset through its end date. If the ratio of snowmelt amount to total rainfall surpasses 0.7, the flood is categorized as snowmelt-driven, otherwise it is regarded as rainfall-driven[5,10]. Furthermore, changes in these two quantified volumes under different warming levels are compared to the baseline period to assess their contribution to flood volume changes. Restricting contributing runoff, rainfall, and snowmelt to the seven days before and during floods may exclude lingering effects from earlier events or soil moisture changes. However, we expect this limitation to have little impact on the main findings of this study. In addition, previous work[5] also indicates the robustness of the related results to the choice of the spatial overlap threshold (e.g., 0.4) and the snowmelt-to-rainfall ratio (e.g., 0.7) used to classify flood types.

Reporting summary

Further information on research design is available in the Nature Portfolio Reporting Summary linked to this article.

References
1. Zscheischler, J. et al. A typology of compound weather and climate events. *Nat. Rev. Earth Environ.* **1**, 333–347 (2020).
2. Kemter, M., Merz, B., Marwan, N., Vorogushyn, S. & Blöschl, G. Joint trends in flood magnitudes and spatial extents across Europe. *Geophys. Res. Lett.* **47**, e2020GL087464 (2020).

3. Jongman, B. et al. Increasing stress on disaster-risk finance due to large floods. *Nat. Clim. Change* **4**, 264–268 (2014).

4. Tradowsky, J. S. et al. Attribution of the heavy rainfall events leading to severe flooding in Western Europe during July 2021. *Clim. Change* **176**, 90 (2023).

5. Fang, B., Bevacqua, E., Rakovec, O. & Zscheischler, J. An increase in the spatial extent of European floods over the last 70 years. *Hydrol. Earth Syst. Sci.* **28**, 3755–3775 (2024).

6. Berghuijs, W. R., Allen, S. T., Harrigan, S. & Kirchner, J. W. Growing spatial scales of synchronous river flooding in Europe. *Geophys. Res. Lett.* **46**, 1423–1428 (2019).

7. Blöschl, G. et al. Changing climate shifts timing of European floods. *Science* **357**, 588–590 (2017).

8. Blöschl, G. et al. Changing climate both increases and decreases European river floods. *Nature* **573**, 108–111 (2019).

9. Jiang, S., Bevacqua, E. & Zscheischler, J. River flooding mechanisms and their changes in Europe revealed by explainable machine learning. *Hydrol. Earth Syst. Sci.* **26**, 6339–6359 (2022).

10. Tarasova, L. et al. Shifts in flood generation processes exacerbate regional flood anomalies in Europe. *Commun. Earth Environ.* **4**, 49 (2023).

11. Berghuijs, W. R., Harrigan, S., Molnar, P., Slater, L. J. & Kirchner, J. W. The relative importance of different flood-generating mechanisms across Europe. *Water Resour. Res.* **55**, 4582–4593 (2019).

12. Blöschl, G. et al. Current European flood-rich period exceptional compared with past 500 years. *Nature* **583**, 560–566 (2020).

13. Lun, D., Fischer, S., Viglione, A. & Blöschl, G. Detecting flood-rich and flood-poor periods in annual peak discharges across Europe. *Water Resour. Res.* **56**, e2019WR026575 (2020).

14. Pendergrass, A. G., Knutti, R., Lehner, F., Deser, C. & Sanderson, B. M. Precipitation variability increases in a warmer climate. *Sci. Rep.* **7**, 17966 (2017).

15. Hosseinzadehtalaei, P., Tabari, H. & Willems, P. Satellite-based data driven quantification of pluvial floods over Europe under future climatic and socioeconomic changes. *Sci. Total Environ.* **721**, 137688 (2020).

16. Hirabayashi, Y. et al. Global flood risk under climate change. *Nat. Clim. Change* **3**, 816–821 (2013).

17. Dankers, R. et al. First look at changes in flood hazard in the inter-sectoral impact model intercomparison project ensemble. *Proc. Natl. Acad. Sci. USA* **111**, 3257–3261 (2014).

18. Tabari, H., Hosseinzadehtalaei, P., Thiery, W. & Willems, P. Amplified drought and flood risk under future socioeconomic and climatic change. *Earth's Future* **9**, e2021EF002295 (2021).

19. Thober, S. et al. Multi-model ensemble projections of European river floods and high flows at 1.5, 2, and 3 degrees global warming. *Environ. Res. Lett.* **13**, 014003 (2018).

20. Di Sante, F., Coppola, E. & Giorgi, F. Projections of river floods in Europe using Euro-Cordex, CMIP5 and CMIP6 simulations. *Int. J. Climatol.* **41**, 3203–3221 (2021).

21. Bertola, M., Viglione, A., Lun, D., Hall, J. & Blöschl, G. Flood trends in Europe: are changes in small and big floods different? *Hydrol. Earth Syst. Sci.* **24**, 1805–1822 (2020).

22. Bertola, M. et al. Do small and large floods have the same drivers of change? A regional attribution analysis in Europe. *Hydrol. Earth Syst. Sci.* **25**, 1347–1364 (2021).

23. Wasko, C., Guo, D., Ho, M., Nathan, R. & Vogel, E. Diverging projections for flood and rainfall frequency curves. *J. Hydrol.* **620**, 129403 (2023).

24. Jiang, S., Tarasova, L., Yu, G. & Zscheischler, J. Compounding effects in flood drivers challenge estimates of extreme river floods. *Sci. Adv.* **10**, eadl4005 (2024).

25. Brunner, M. I. & Gilleland, E. Future changes in floods, droughts, and their extents in the Alps: a sensitivity analysis with a non-stationary stochastic streamflow generator. *Earth's Future* **12**, e2023EF004238 (2024).

26. Griffin, A. et al. Widespread flooding dynamics under climate change: characterising floods using grid-based hydrological modelling and regional climate projections. *Hydrol. Earth Syst. Sci.* **28**, 2635–2650 (2024).

27. Zscheischler, J., Mahecha, M. D., Harmeling, S. & Reichstein, M. Detection and attribution of large spatiotemporal extreme events in earth observation data. *Ecol. Inform.* **15**, 66–73 (2013).

28. Paprotny, D., Morales-Nápoles, O. & Jonkman, S. N. Hanze: a pan-european database of exposure to natural hazards and damaging historical floods since 1870. *Earth Syst. Sci. Data* **10**, 565–581 (2018).

29. United Nations Framework Convention on Climate Change (UNFCCC). *Paris Agreement*. FCCC/CP/2015/L.9/Rev.1. Adopted on 12 December 2015 at the 21st Conference of the Parties (COP21) in Paris, France. (2015).

30. Masson-Delmotte, V. et al. *Climate Change 2021: the Physical Science Basis. Contribution of Working Group I to the Sixth Assessment Report of the Intergovernmental Panel on Climate Change* (Cambridge University Press, 2021).

31. Vormoor, K., Lawrence, D., Heistermann, M. & Bronstert, A. Climate change impacts on the seasonality and generation processes of floods & projections and uncertainties for catchments with mixed snowmelt/rainfall regimes. *Hydrol. Earth Syst. Sci.* **19**, 913–931 (2015).

32. Räisänen, J. Snow conditions in northern Europe: the dynamics of interannual variability versus projected long-term change. *Cryosphere* **15**, 1677–1696 (2021).

33. Barcikowska, M. J. et al. Changes in the future summer mediterranean climate: contribution of teleconnections and local factors. *Earth Syst. Dyn.* **11**, 161–181 (2020).

34. Huo, R. et al. Extreme precipitation changes in Europe from the last millennium to the end of the twenty-first century. *J. Clim.* **34**, 567–588 (2021).

35. Rottler, E., Bronstert, A., Bürger, G. & Rakovec, O. Projected changes in Rhine River flood seasonality under global warming. *Hydrol. Earth Syst. Sci.* **25**, 2353–2371 (2021).

36. Wasko, C., Nathan, R. & Peel, M. C. Trends in global flood and streamflow timing based on local water year. *Water Resour. Res.* **56**, e2020WR027233 (2020).

37. Chemke, R., Zanna, L., Orbe, C., Sentman, L. T. & Polvani, L. M. The future intensification of the North Atlantic winter storm track: the key role of dynamic ocean coupling. *J. Clim.* **35**, 2407–2421 (2022).

38. Alfieri, L., Dottori, F., Betts, R., Salamon, P. & Feyen, L. Multi-model projections of river flood risk in Europe under global warming. *Climate* **6**, 6 (2018).

39. Roudier, P. et al. Projections of future floods and hydrological droughts in Europe under a +2 °C global warming. *Clim. Change* **135**, 341–355 (2016).

40. Zhang, S. et al. Reconciling disagreement on global river flood changes in a warming climate. *Nat. Clim. Change* **12**, 1160–1167 (2022).

41. Arnell, N. W. & Gosling, S. N. The impacts of climate change on river flood risk at the global scale. *Clim. Change* **134**, 387–401 (2016).

42. Blum, A. G., Ferraro, P. J., Archfield, S. A. & Ryberg, K. R. Causal effect of impervious cover on annual flood magnitude for the United States. *Geophys. Res. Lett.* **47**, e2019GL086480 (2020).

43. Jovanovic, T., Mejía, A., Gall, H. & Gironás, J. Effect of urbanization on the long-term persistence of streamflow records. *Phys. A* **447**, 208–221 (2016).

44. Prosdocimi, I., Kjeldsen, T. R. & Miller, J. D. Detection and attribution of urbanization effect on flood extremes using nonstationary flood-frequency models. *Water Resour. Res.* **51**, 4244–4262 (2015).

45. Zhang, W., Villarini, G., Vecchi, G. A. & Smith, J. A. Urbanization exacerbated the rainfall and flooding caused by hurricane Harvey in Houston. *Nature* **563**, 384–388 (2018).

46. Slater, L. J. et al. Nonstationary weather and water extremes: a review of methods for their detection, attribution, and management. *Hydrol. Earth Syst. Sci.* **25**, 3897–3935 (2021).

47. Taylor, K. E., Stouffer, R. J. & Meehl, G. A. An overview of CMIP5 and the experiment design. *Bull. Am. Meteorol. Soc.* **93**, 485–498 (2012).

48. Frieler, K. et al. Assessing the impacts of 1.5 °C global warming–simulation protocol of the inter-sectoral impact model intercomparison project (isimip2b). *Geosci. Model Dev.* **10**, 4321–4345 (2017).

49. Ito, R., Shiogama, H., Nakaegawa, T. & Takayabu, I. Uncertainties in climate change projections covered by the ISIMIP and CORDEX model subsets from CMIP5. *Geosci. Model Dev.* **13**, 859–872 (2020).

50. Samaniego, L. et al. Hydrological forecasts and projections for improved decision-making in the water sector in Europe. *Bull. Am. Meteorol. Soc.* **100**, 2451–2472 (2019).

51. Zelinka, M. D. et al. Causes of higher climate sensitivity in CMIP6 models. *Geophys. Res. Lett.* **47**, e2019GL085782 (2020).

52. Hirabayashi, Y., Tanoue, M., Sasaki, O., Zhou, X. & Yamazaki, D. Global exposure to flooding from the new CMIP6 climate model projections. *Sci. Rep.* **11**, 3740 (2021).

53. Kim, Y.-H., Min, S.-K., Zhang, X., Sillmann, J. & Sandstad, M. Evaluation of the CMIP6 multi-model ensemble for climate extreme indices. *Weather Clim. Extrem.* **29**, 100269 (2020).

54. Fuentes-Franco, R., Docquier, D., Koenigk, T., Zimmermann, K. & Giorgi, F. Winter heavy precipitation events over Northern Europe modulated by a weaker NAO variability by the end of the 21st century. *npj Clim. Atmos. Sci.* **6**, 72 (2023).

55. European Parliament and Council of the European Union. Directive 2007/60/EC of 23 October 2007 on the assessment and management of flood risks. *Off. J. Eur. Union.* **L288**, 27–34 (2007).

56. Merz, B. et al. Floods and climate: emerging perspectives for flood risk assessment and management. *Nat. Hazards Earth Syst. Sci.* **14**, 1921–1942 (2014).

57. Dottori, F. et al. Increased human and economic losses from river flooding with anthropogenic warming. *Nat. Clim. Change* **8**, 781–786 (2018).

58. Vousdoukas, M. I. et al. Climatic and socioeconomic controls of future coastal flood risk in Europe. *Nat. Clim. Change* **8**, 776–780 (2018).

59. Kumar, R., Samaniego, L. & Attinger, S. Implications of distributed hydrologic model parameterization on water fluxes at multiple scales and locations. *Water Resour. Res.* **49**, 360–379 (2013).

60. Samaniego, L., Kumar, R. & Attinger, S. Multiscale parameter regionalization of a grid-based hydrologic model at the mesoscale. *Water Resour. Res.* **46**, W05523 (2010).

61. Hempel, S., Frieler, K., Warszawski, L., Schewe, J. & Piontek, F. A trend-preserving bias correction–the ISI-MIP approach. *Earth Syst. Dyn.* **4**, 219–236 (2013).

62. Wood, E. F. et al. Hyperresolution global land surface modeling: meeting a grand challenge for monitoring Earth's terrestrial water. *Water Resour. Res.* **47**, https://agupubs.onlinelibrary.wiley.com/doi/pdf/10.1029/2010WR010090 (2011).

63. Bierkens, M. F. P. et al. Hyper-resolution global hydrological modelling: what is next? *Hydrol. Process.* **29**, 310–320 (2015).

64. Metzger, M. J., Bunce, R. G. H., Jongman, R. H. G., Mücher, C. A. & Watkins, J. W. A climatic stratification of the environment of Europe. *Glob. Ecol. Biogeogr.* **14**, 549–563 (2005).

65. Marx, A. et al. Climate change alters low flows in Europe under global warming of 1.5, 2, and 3 °. *Hydrol. Earth Syst. Sci.* **22**, 1017–1032 (2018).

66. Bertola, M. et al. Megafloods in Europe can be anticipated from observations in hydrologically similar catchments. *Nat. Geosci.* **16**, 982–988 (2023).

67. Stein, L., Pianosi, F. & Woods, R. Event-based classification for global study of river flood generating processes. *Hydrol. Process.* **34**, 1514–1529 (2020).

68. Hall, J. & Blöschl, G. Spatial patterns and characteristics of flood seasonality in Europe. *Hydrol. Earth Syst. Sci.* **22**, 3883–3901 (2018).

Author contributions
B.F. and J.Z. conceived the study. B.F. performed all analyses and wrote the initial draft. E.B. contributed to the interpretation of the results. O.R. and R.K. conducted the mHM simulations and helped with the interpretation. All authors substantially contributed to the final draft.

Competing interests
The authors declare no competing interests.

Additional information
Supplementary information The online version contains supplementary material available at https://doi.org/10.1038/s43247-025-02734-y.

Correspondence and requests for materials should be addressed to Beijing Fang.

Peer review information *Communications Earth & Environment* thanks Ruhhee Tabassum and the other anonymous reviewer(s) for their contribution to the peer review of this work. Primary handling editors: Rajarshi Das Bhowmik and Alireza Bahadori. A peer review file is available.

Reprints and permissions information is available at http://www.nature.com/reprints

Publisher's note Springer Nature remains neutral with regard to jurisdictional claims in published maps and institutional affiliations.